forum acusticum 2023

# SIMULATION OF THE SNARE-MEMBRANE COLLISION IN MODAL FORM USING THE SCALAR AUXILIARY VARIABLE (SAV) METHOD

**Michele Ducceschi*** **Matthew Hamilton** **Riccardo Russo**
Department of Industrial Engineering, University of Bologna, Italy

## ABSTRACT

Collisions play an essential role in the sound production of many musical instruments, such as in the snare drum. Here, collisions occur between the stick and the batter head and between the snares and the bottom head. The latter involve interactions between fully distributed objects and are the subject of this work. From a simulation standpoint, simple explicit or semi-implicit schemes are prone to unstable numerical behaviour and an appropriate energy-conserving framework is required for stable simulation designs. Usually, this is accomplished via fully-implicit designs that are known to conserve energy but that require iterative solvers such as Newton-Raphson. Other than representing a computational bottleneck, iterative schemes present a variable operational cost per time-step and, furthermore, are serial in nature. This work will explore the possibility of simulating the snare-membrane collision using explicit designs obtained via a quadratisation of the nonlinear potential energy. A modal function basis will be employed for the spatial discretisation, allowing for fine-tuning damping ratios and natural frequencies.

**Keywords:** *snare drum, collision modelling, energy methods, physical modelling, Scalar Auxiliary Variable (SAV)*

## 1. INTRODUCTION

A snare drum is a percussion instrument of cylindrical geometry, composed of a top membrane (the batter) and a bottom membrane along with a rattle of thin wires (the snares). Air is enclosed between the membranes and a rigid rim, serving as the resonant cavity across which vibrations are transmitted between the two membranes. The wires serve as rattling elements colliding against the bottom membrane, causing the typical sharp tone of the snare drum. In this work the modelling and simulation of the snare-membrane interaction is discussed. Physics-based simulation of the snare drum has been the subject of various works by Bilbao and associates [1, 2]. Compared to the works of Bilbao, the equations here will be solved in the modal domain, yielding a rather convenient framework in which the decay times and the resonant frequencies may be finely tuned.

The collision may be realised at the modelling level by employing a one-sided power law yielding a non-zero force when the objects are in contact. This model, used in several previous works (see. e.g. [3–5]) reproduces the most prevalent perceptual features of collisions. Furthermore, it may be derived from a nonlinear potential as a function of the collision deformation. Conveniently, energy conservation yields a natural framework to bound the growth of the solutions over time, resulting in a form of stability [6].

At the simulation level, simple numerical designs display unpredictable and unstable numerical behaviour due to the strongly nonlinear character of the collision dynamics. Much effort has been dedicated to the realisation of energy-stable schemes mimicking the conservation property of the continuous system and ensuring the stability of the time-stepping routine. An application of one such method, the Scalar Auxiliary Variable (SAV) approach [7], is illustrated in this work. For the SAV, the nonlinear energy is first quadratised by means of an auxiliary state function. The resulting numerical schemes are then updated explicitly in time [8]. Due to their remarkable efficiency, the schemes are particularly attractive from the

**Corresponding author*: michele.ducceschi@unibo.it.

standpoint of real-time simulation and are currently seeing a growing body of applications in physics-based sound synthesis [9–11].

## 2. CONTINUOUS MODELS

In this section, the case of the collision of a wire against a membrane is discussed. This serves as the basic building block of the full snare drum, to be addressed later. The system is here written as:

$$\varrho\,\partial_t^2 u(z,t) = T\,\partial_z^2 u(z,t) + f(\eta), \tag{1a}$$

$$\rho\,\partial_t^2 w(\mathbf{x},t) = P\,\Delta w(\mathbf{x},t) - \beta(\mathbf{x}) f(\eta). \tag{1b}$$

Here, $u, w$ represent the physical displacements of the wire and the membrane, respectively. Both systems are defined for $t \geq 0$. The wire is spatially distributed along $\mathcal{F} : \{z \,|\, z \in [-L/2, L/2]\}$, whereas the membrane occupies a circular domain $\mathcal{G} : \{\mathbf{x} := (r\cos\theta, r\sin\theta) \,|\, 0 \leq r \leq R,\ 0 \leq \theta \leq 2\pi\}$. It is assumed that $\mathcal{F} \subset \mathcal{G}$, see Figure 1. The symbol $\partial_m^n$ denotes the $n^{\text{th}}$ partial derivative with respect to $m$; $\Delta$ is the two-dimensional Laplace operator. Constants appear as: $\varrho$, the linear density of the wire; $\rho$, the surface density of the membrane; $T$ the tension applied to the string's ends; $P$ the tension per unit length applied to the membrane's edge.

The interaction collision force density $f$ (in $\mathrm{N}\cdot\mathrm{m}^{-1}$) is defined as:

$$f = \frac{\mathrm{d}\phi}{\mathrm{d}\eta} := \frac{\mathrm{d}}{\mathrm{d}\eta}\left(\frac{B[\eta]_+^{\alpha+1}}{\alpha+1}\right),\ [\eta]_+ := \frac{\eta + |\eta|}{2}, \tag{2}$$

where $\alpha \geq 1$ is a nonlinear exponent, and $B \geq 0$ is a stiffness constant. Above, $[\eta]_+$ is the *positive part* of $\eta$ (identically zero for $\eta \leq 0$), identifying a one-sided interaction between the colliding wire and membrane. Conveniently, $\eta$ is identified as the inter-object collision deformation:

$$\eta := \int_{\mathcal{G}} \beta(\mathbf{x}) w(\mathbf{x},t)\mathrm{d}\mathbf{x} - u(z,t). \tag{3}$$

The distribution $\beta$, appearing in the definition of $\eta$ as well as in (1b), is a kind of projector of $\mathcal{G}$ onto $\mathcal{F}$, given as:

$$\int_{\mathcal{G}} \beta(\mathbf{x}) f(\mathbf{x})\mathrm{d}\mathbf{x} := \int_{\mathcal{F}} f(z)\mathrm{d}z = \int_{-L/2}^{L/2} f(z)\mathrm{d}z, \tag{4}$$

thus effectively yielding $\eta = w(z,t) - u(z,t)$.

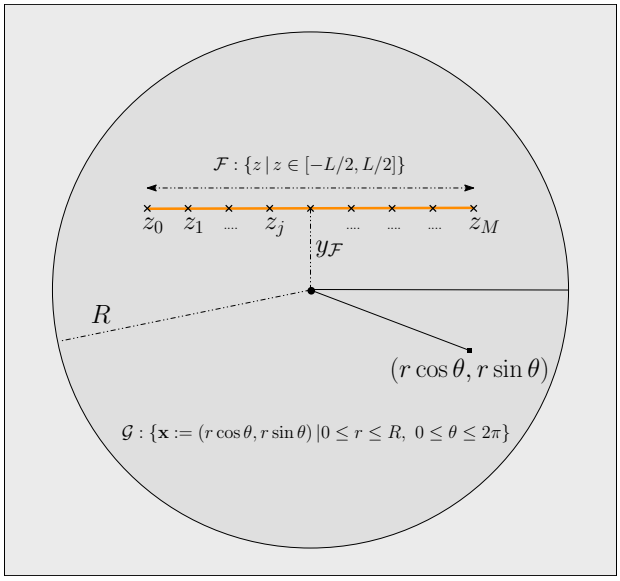


**Figure 1**. Domains of definition of the wire and membrane. The wire is represented as an orange line. It is assumed that $\mathcal{F} \subset \mathcal{G}$. The discrete grid, used in the calculation of the nonlinear integral (12) is also illustrated.

### 2.1 Energy conservation

System (1) is conservative. While losses are necessary for realistic sound synthesis, it is convenient to derive an energy-conservation property in the lossless case. Doing so will serve as the basis to prove the stability of the proposed time-stepping scheme. By adding losses in the modal domain, one can effortlessly set a fine frequency-dependent damping profile at no additional cost, as will be discussed in Section 6. Energy conservation is derived by multiplying (1a) by $\partial_t u$ and integrating over $\mathcal{F}$, and by multiplying (1b) by $\partial_t w$ and integrating over $\mathcal{G}$. After integration by parts, and by means of definitions (2), (3), (4), one obtains the following energy balance:

$$\frac{\mathrm{d}H}{\mathrm{d}t} := \frac{\mathrm{d}(H_u + H_w + H_\eta)}{\mathrm{d}t} = 0, \tag{5}$$

where the energy components for the wire, membrane and collision are given as:

$$H_u = \int_{\mathcal{F}} \left( \frac{\varrho}{2}(\partial_t u)^2 + \frac{T}{2}(\partial_z u)^2 \right) \mathrm{d}z, \tag{6a}$$

$$H_w = \int_{\mathcal{G}} \left( \frac{\rho}{2}(\partial_t w)^2 + \frac{P}{2}|\nabla w|^2 \right) \mathrm{d}\mathbf{x}, \tag{6b}$$

$$H_\eta = \int_{\mathcal{F}} \phi \, \mathrm{d}z. \tag{6c}$$

The energy balance above holds under a suitable set of boundary conditions, which are assumed to be of Dirichlet type for both the wire and the membrane:

$$u(z,t)|_{z=\pm L/2} = w(\mathbf{x},t)|_{r=R} = 0, \quad \forall t \geq 0. \tag{7}$$

## 3. MODAL EQUATIONS

The energy components above are now computed using the modes, which give a set of time-dependent relations depending exclusively on the modal coordinates. To that end, consider the following expansion for the wire and membrane displacements:

$$u = \mathbf{U}^\intercal(z)\mathbf{a}(t), \quad w = \mathbf{W}^\intercal(\theta, r)\mathbf{b}(t), \tag{8}$$

where $\mathbf{a}$, $\mathbf{b}$ are the modal coordinates, functions of time only. The upper bounds in the summations (8) are given as $N_u$, $N_w$, respectively and are fixed by Nyquist requirements, as will be shown in Section 4. Here, the normalised modal shapes are given as [12]:

$$U_p := \sqrt{\frac{2}{L}} \sin \frac{p\pi(z + L/2)}{L}, \tag{9a}$$

$$W_p := A_{p^\theta,p^r} \begin{Bmatrix} \cos(p^\theta \theta) \\ \sin(p^\theta \theta) \end{Bmatrix} J_{p^\theta}\left(\mu_{p^\theta,p^r} \frac{r}{R}\right). \tag{9b}$$

where $p, p^r \in \mathbb{N}$, and $p^\theta \in \mathbb{N} \cup \{0\}$. Above, $A_{p^\theta,p^r}$ is a convenient normalisation constant, given as:

$$A_{p^\theta,p^r} := \sqrt{\frac{c(p^\theta)}{R^2 \pi J^2_{p^\theta+1}(\mu_{p^\theta,p^r})}},$$

where $c = 1$ if $p^\theta = 0$, and 2 otherwise. The double index in the expression in $W_p$ reflects the fact that, for the $p$th membrane mode, two modal indices $p^r, p^\theta$ (radial and angular) are necessary to specify the mode. Note as well that, in the expression for $W_p$ above, modal degeneracy is encoded as a double trigonometric function within the curly brackets. Furthermore, $\mu_{p^\theta,p^r}$ represents the $p^r$th zero of the Bessel function of the first kind $J_{p^\theta}$. Inserting the modal expansions in (6a) and (6b) using $\mathrm{d}\mathbf{x} = r\mathrm{d}r\mathrm{d}\theta$, the integrals may be computed directly, yielding:

$$H_u = \frac{\varrho}{2} \dot{\mathbf{a}}^\intercal \dot{\mathbf{a}} + \frac{1}{2} \mathbf{a}^\intercal \mathbf{A}\, \mathbf{a}, \tag{10a}$$

$$H_w = \frac{\rho}{2} \dot{\mathbf{b}}^\intercal \dot{\mathbf{b}} + \frac{1}{2} \mathbf{b}^\intercal \mathbf{B}\, \mathbf{b}. \tag{10b}$$

Note that the dot notation is used for indicating total time derivatives in the modal domain, replacing partial differentiation in the time domain. Above, $\mathbf{A}$, $\mathbf{B}$ are positive, diagonal matrices containing the eigenvalues of the wire and the membrane, respectively, in ascending order. These are defined as:

$$[\mathbf{A}]_{p,p} := T\left(\frac{p\pi}{L}\right)^2, \quad [\mathbf{B}]_{p,p} := P\left(\frac{\mu_{p^\theta,p^r}}{R}\right)^2. \tag{11}$$

A discretisation of (6c) is also required. As a result of the nonlinear character of $\phi$, the integral cannot be computed directly. Instead, the integral is evaluated on a grid of points, as:

$$H_\eta \approx \frac{L}{M} \sum_{j=0}^{M} \phi(\eta_j), \tag{12}$$

for a number of grid intervals $M$ to be specified later. Furthermore:

$$\eta_j := w(z_j,t) - u(z_j,t), \quad z_j := \frac{jL}{M}, \tag{13}$$

see also Figure 1.

### 3.1 Energy quadratisation

In view of the SAV approach shown below, it is useful to "quadratise" the nonlinear energy, such that

$$\psi := \sqrt{2H_\eta} = \sqrt{\frac{2L}{M} \sum_{j=0}^{M} \phi(\eta_j)}. \tag{14}$$

The total energy in the modal domain is thus given by:

$$H = H_u + H_w + \frac{\psi^2}{2}, \tag{15}$$

where $H_u$ and $H_w$ have the forms (10a), (10b) respectively. Note that the total energy is a function of the modal coordinates $\mathbf{a}, \mathbf{b}$ only, and includes only quadratic terms.

The modal equations can therefore be derived by differentiating appropriately the expression of the energy according to $\mathbf{a}, \mathbf{b}$. Thus:

$$\varrho\, \ddot{\mathbf{a}} = -\mathbf{A}\mathbf{a} + \psi \nabla_{\mathbf{a}} \psi, \tag{16a}$$

$$\rho\, \ddot{\mathbf{b}} = -\mathbf{B}\mathbf{b} + \psi \nabla_{\mathbf{b}} \psi. \tag{16b}$$

The time variation of the auxiliary variable is:

$$\dot{\psi} = (\nabla_{\mathbf{a}} \psi)^{\mathsf{T}}\, \dot{\mathbf{a}} + (\nabla_{\mathbf{b}} \psi)^{\mathsf{T}}\, \dot{\mathbf{b}}. \tag{17}$$

### 3.2 Hamiltonian formulation

System (16), along with the rate of change of $\psi$, can be written compactly as an augmented Hamiltonian system:

$$\dot{\mathbf{q}} = \mathbf{M}^{-1}\mathbf{p}, \tag{18a}$$

$$\dot{\mathbf{p}} = -\mathbf{K}\mathbf{q} - \psi \mathbf{g}, \tag{18b}$$

$$\dot{\psi} = \mathbf{g}^{\mathsf{T}}\mathbf{M}^{-1}\mathbf{p}, \tag{18c}$$

for the generalised coordinates $\mathbf{q} := [\mathbf{a}^{\mathsf{T}}, \mathbf{b}^{\mathsf{T}}]^{\mathsf{T}}$ and momenta $\mathbf{p}$. The mass and stiffness matrices are given as:

$$\mathbf{M} = \begin{bmatrix} \varrho\, \mathbf{I}_{N_u} & \mathbf{0} \\ \mathbf{0} & \rho\, \mathbf{I}_{N_w} \end{bmatrix}, \quad \mathbf{K} = \begin{bmatrix} \mathbf{A} & \mathbf{0} \\ \mathbf{0} & \mathbf{B} \end{bmatrix}, \tag{19}$$

with $\mathbf{I}_N$ being the $N \times N$ identity matrix. Note that both matrices are fully diagonal. Furthermore:

$$\mathbf{g} := [(\nabla_{\mathbf{a}} \psi)^{\mathsf{T}}, (\nabla_{\mathbf{b}} \psi)^{\mathsf{T}}]^{\mathsf{T}}. \tag{20}$$

Note that system (18) is linear in $\mathbf{p}$, $\mathbf{q}$, $\psi$, if $\mathbf{g}$ is assumed known at all times. Here, $\mathbf{g}$ contains all the nonlinearities. This is a key feature of the current formulation, allowing to design the fast time-stepping formulation given below. Before proceeding, it is worth writing the form of the energy in this formulation:

$$H = \frac{1}{2}\mathbf{p}^{\mathsf{T}}\mathbf{M}^{-1}\mathbf{p} + \frac{1}{2}\mathbf{q}^{\mathsf{T}}\mathbf{K}\mathbf{q} + \frac{\psi^2}{2}. \tag{21}$$

This expression is the same as (15), though given in terms of the Hamiltonian coordinates and momenta, $\psi$ being itself a function of $\mathbf{q}$, via (14). System (18) is a compact representation of the equations of motion (1), and lends itself to an energy-stable and efficient time-stepping routine, which will be presented shortly. Output is extracted by first calculating $\mathbf{q}$ (and, thus, $\mathbf{a}$ and $\mathbf{b}$). Then, the physical displacement of the wire and of the membrane are reconstructed at the desired locations via (8).

## 4. TIME DISCRETISATION

Time is now discretised along a time grid, with constant time step $k$, via the time series $\mathbf{q}^n$, $\mathbf{p}^{n-\frac{1}{2}}$, $\psi^{n-\frac{1}{2}}$. These are evaluated at the times $t_n := kn$, $t_{n-\frac{1}{2}} := k(n-\frac{1}{2})$, where $n \in \mathbb{N}$ is the time index, and are to be considered approximations to the continuous solutions $\mathbf{q}(t_n)$, $\mathbf{p}(t_{n-\frac{1}{2}})$, $\psi(t_{n-\frac{1}{2}})$. A discretisation of (18) follows as:

$$\mathbf{q}^{n+1} = \mathbf{q}^n + k\mathbf{M}^{-1}\mathbf{p}^{n+\frac{1}{2}}, \tag{22a}$$

$$\mathbf{p}^{n+\frac{1}{2}} = \mathbf{p}^{n-\frac{1}{2}} - \tfrac{k}{2}\mathbf{g}^n \left( \psi^{n+\frac{1}{2}} + \psi^{n-\frac{1}{2}} \right), \tag{22b}$$

$$\psi^{n+\frac{1}{2}} = \psi^{n-\frac{1}{2}} + \tfrac{1}{2} \left(\mathbf{g}^n\right)^{\mathsf{T}} \left( \mathbf{q}^{n+1} - \mathbf{q}^{n-1} \right). \tag{22c}$$

Note that the nonlinearities, encoded in the vector $\mathbf{g}$, are computed at previous time steps, and can therefore be explicitly evaluated at all times. After a few algebraic manipulations, the update takes the form

$$\mathbf{Q}^n \mathbf{q}^{n+1} = \mathbf{y}^n, \tag{23}$$

where

$$\mathbf{Q}^n = \mathbf{I} + \boldsymbol{\gamma}^n (\boldsymbol{\kappa}^n)^{\mathsf{T}},$$

$$\mathbf{y}^n = 2\mathbf{q}^n - 2k\boldsymbol{\gamma}^n \psi^{n-\frac{1}{2}} - \left(\mathbf{I} - \boldsymbol{\gamma}^n (\boldsymbol{\kappa}^n)^{\mathsf{T}}\right) \mathbf{q}^{n-1}.$$

The vectors $\boldsymbol{\gamma}^n$ and $\boldsymbol{\kappa}^n$ are defined in terms of $\mathbf{g}^n$ by $\boldsymbol{\gamma}^n = \frac{k}{2}\mathbf{M}^{-1}\mathbf{g}^n$ and $\boldsymbol{\kappa}^n = \frac{k}{2}\mathbf{g}^n$. Thus, given $\mathbf{q}^n$, $\mathbf{q}^{n-1}$ and $\psi^{n-\frac{1}{2}}$, both $\mathbf{Q}^n$ and $\mathbf{y}^n$ are known. Once $\mathbf{q}^{n+1}$ is computed, $\psi$ is updated immediately via (22c). The system matrix $\mathbf{Q}$ is dense, but invertible in $\mathcal{O}(N_u + N_w)$ operations using the Sherman-Morrison formula [13], yielding compute times on par with those of simpler, yet unstable designs such as Störmer-Verlet; see [8]. Furthermore, a form of the discrete energy is conserved as:

$$H = \tfrac{1}{2} \left( \mathbf{p}^{n+\frac{1}{2}} \right)^{\mathsf{T}} \mathbf{M}^{-1} \mathbf{p}^{n+\frac{1}{2}} + \\ + \tfrac{1}{2} (\mathbf{q}^{n+1})^{\mathsf{T}} \mathbf{K} \mathbf{q}^n + \tfrac{1}{2} \left( \psi^{n+\frac{1}{2}} \right)^2, \tag{24}$$

clearly discretising (21). As opposed to the continuous-time energy, though, a condition here arises for the non-negativity of the energy overall. Following [8], this is given as:

$$k \leq \frac{2}{\lambda_{\max} \left( \mathbf{M}^{-\frac{1}{2}} \mathbf{K} \mathbf{M}^{-\frac{T}{2}} \right)}. \tag{25}$$

in terms of the largest system eigenvalue $\lambda_{\max}$. This is easily related to the eigenfrequencies, and hence to the eigenvalues of the wire and the membrane, given in (11), fixing the upper limits $N_u$, $N_w$ of the system's modes. When the energy overall is non-negative, stability ensues, and thus (25) may be regarded as a sufficient condition for stability.

The form of $\mathbf{g}^n$ is analytic, as per (20). One only needs to evaluate the continuous-time gradients at the time $t = t_n$. In component form, the analytic expressions of the gradients are given by:

$$(\nabla_{\mathbf{a}}\psi)_p := \frac{LB}{\psi M}\sum_{j=0}^{M}[\eta_j]_+^{\alpha}(-U_p(z_j)), \tag{26a}$$

$$(\nabla_{\mathbf{b}}\psi)_p := \frac{LB}{\psi M}\sum_{j=0}^{M}[\eta_j]_+^{\alpha}(W_p(z_j)). \tag{26b}$$

Note that these expressions should be set to zero when $\eta_j \leq 0\ \forall j$. Finally, a question arises as how to select $M$, the number of grid intervals of the domain $\mathcal{F}$. One option is to divide $\mathcal{F}$ using the Courant–Friedrichs–Lewy (CFL) condition for the wave equation [6], such that, for a given time step $k$, one has

$$M \approx \sqrt{\frac{\varrho}{T}}\frac{L}{k}. \tag{27}$$

The exact value of $M$ may be found by rounding the above to the nearest integer.

## 5. NUMERICAL EXAMPLES

The extremely compact form of (22), combined with its remarkable efficiency and provable stability, has led to the real-time simulation of systems that were out-of-reach with previous simulation designs, including the von Kármán plate equations [11], the geometrically exact nonlinear piano string [9], and networks with thousands of nonlinearly coupled degrees of freedom [10].

As an illustrative example, consider Figure 2 where the wire is released from its first mode of vibration. During collision, energy is exchanged between the wire and the membrane, and wavefronts appear on the surface of the membrane. Note that the whole dynamics is here solved *explicitly*, via (22), yet the resulting simulation is stable in spite of the strong nonlinearity introduced by the collision potential. A check of the numerical energy conservation is given in Figure (3), where the energy components as well as the energy error are plotted, showing conservation of energy to a very small value.

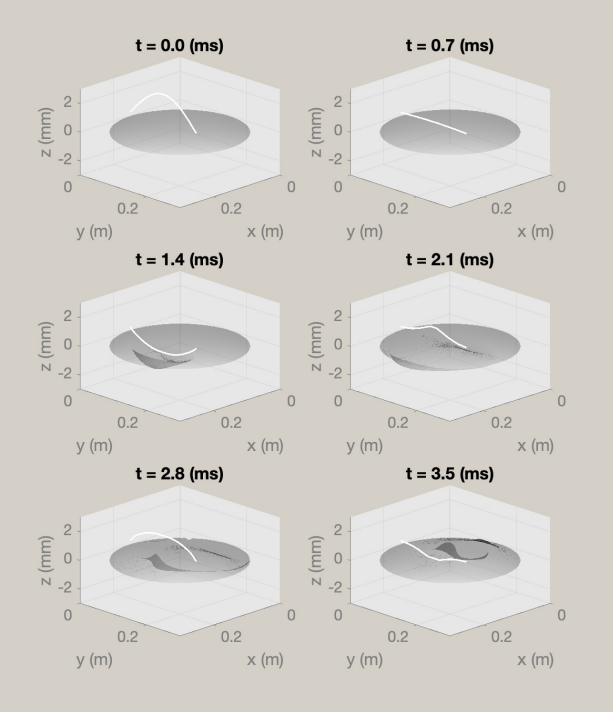


**Figure 2**. Snapshots of the wire-membrane interaction. Here, the membrane has a radius $R = 0.15$ m, $\rho = 0.2$ kg $\cdot$ m$^{-2}$, $P = 2000$ N $\cdot$ m$^{-1}$. The wire has $L = 0.2$ m, $\varrho = 1.6 \cdot 10^{-3}$ kg $\cdot$ m$^{-1}$, $T = 30$ N, and $y_{\mathcal{F}} = 5$ cm (for the definition of $y_{\mathcal{F}}$, see Figure 1). The wire is sitting 1 mm above the membrane in its rest position. The collision parameters are selected as $B = 10^{10}$, $\alpha = 1.1$. The system is initialised in the wire's first mode, with an amplitude of 2 mm. Here, $k = 1/(44100 \cdot 5)$.

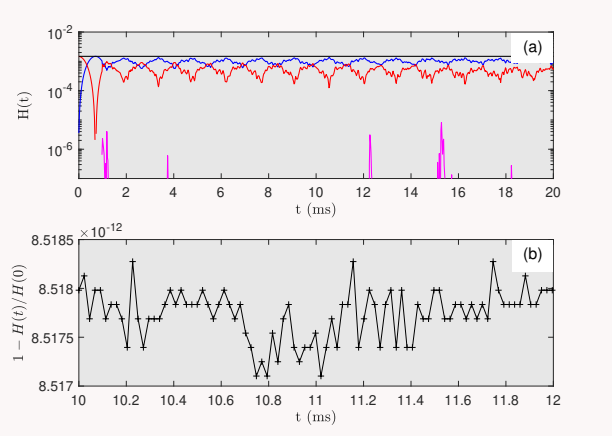


**Figure 3**. Energy plots for the wire and membrane of Figure 2. (a). Energy components (blue: kinetic; red: linear potential; magenta: collision; black: total). (b). Energy error.

## 6. EXTENSIONS

Model (1) is too crude for realistic synthesis. Ideally, a full-scale model should include the two membranes, the air cavity coupling them, a whole set of snares rather than just a single wire as here, an input force and of course losses. These points are now addressed.

The inclusion of a set of snares is a trivial extension of what was already presented here, and will not be discussed further.

The inclusion of an input force may be done in two ways: one is by adding a simple wideband signal in a feedforward manner (as done in countless previous works in sound synthesis [6]), and including tunable amplitude and duration parameters; a second strategy is to model the collision of the stick and the batter head using a collision model analogous to the one employed here, for increased accuracy and control.

The inclusion of a second membrane and the air cavity could follow the development in [1] using finite differences. In the modal domain, a complication arises as the modes of the coupled membrane and air cavity are not easily available in closed-form. An approach consists of discretising in space the continuous equation using finite differences, producing a basis of modal functions via a generalised eigenvalue problem, as done in previous works [14]. Arguably, the modes and related frequencies would be affected by an error due to the numerical approximation, casting doubts on the use of the modal approach in this case. However, note that the eigenvalue problem could be solved offline using a very fine mesh, attenuating the effects of the numerical error. Only the modes satisfying the Nyquist requirements, as per (25), should be kept.

The modal domain is particularly attractive in that the resonant frequencies as well as the modal decay times can be finely tuned. Arbitrarily replacing the numerical eigenvalues with custom values following perceptual considerations, or calibrated on measured responses would greatly benefit the resulting synthesis. The same argument can be made for the losses, responsible for a great deal of perceptually meaningful features. The modal equation may be further reduced by means of Reduced Order Models (ROMs) [15], again building upon perceptual and physical considerations, considerably speeding up the synthesis process.

## 7. CONCLUSIONS

This work presented a model for the nonlinear interaction of a thin wire and a membrane by means of a one-sided collision potential. An energy-consistent modal framework was developed, allowing to write the resulting time-dependent equation in a form amenable to an augmented Hamiltonian system for which a fast, energy-stable simulation routine exists as an application of the recent Scalar Auxiliary Variable (SAV) method. The theoretical framework was compounded by a numerical illustration, showing the ability of the proposed method to solve the system's dynamics in a stable manner. Conditions for numerical stability were given as a function of the system's eigenvalues. Extensions of the proposed model, necessary for realistic synthesis, were discussed and are left as future work.

## 8. ACKNOWLEDGMENTS

This work was supported by the European Research Council (ERC), under grant 2020-StG-950084-NEMUS.

## 9. REFERENCES

[1] S. Bilbao, "Time domain simulation and sound synthesis for the snare drum," *J. Acoust. Soc. Am.*, vol. 131, pp. 914–25, 01 2012.

[2] A. Torin, B. Hamilton, and S. Bilbao, "An energy conserving finite difference scheme for the simulation of

collisions in snare drums," in *Proc. Digital Audio Effects (DAFx-14)*, (Erlangen, Germany), 01 2014.

[3] V. Chatziioannou and M. Van Walstijn, "Energy conserving schemes for the simulation of musical instrument contact dynamics," *J. Sound Vib.*, vol. 339, pp. 262–279, 03 2015.

[4] S. Bilbao, A. Torin, and V. Chatziioannou, "Numerical modeling of collisions in musical instruments," *Acta Acust. United Acust.*, vol. 101, no. 1, pp. 155–173, 2015.

[5] M. Ducceschi, S. Bilbao, S. Willemsen, and S. Serafin, "Linearly-implicit schemes for collisions in musical acoustics based on energy quadratisation," *J. Acoust. Soc. Am.*, vol. 149, pp. 3502–3516, 05 2021.

[6] S. Bilbao, *Numerical sound synthesis: finite difference schemes and simulation in musical acoustics*. Chichester, UK: John Wiley & Sons, 2009.

[7] J. Shen, J. Xu, and J. Yang, "The scalar auxiliary variable (sav) approach for gradient flows," *J. Comput. Phys.*, vol. 353, pp. 407–416, 2018.

[8] S. Bilbao, M. Ducceschi, and F. Zama, "Explicit exactly energy-conserving methods for hamiltonian systems," *J. Comput. Phys.*, vol. 472, p. 111697, 2023.

[9] M. Ducceschi, S. Bilbao, and C. Webb, "Real-time simulation of the struck piano string with geometrically exact nonlinearity via novel quadratic hamiltonian method," in *Proc. European Nonlinear Dyn. Conf. ENOC2020*, (Lyon, France), 07 2022.

[10] M. Ducceschi, S. Bilbao, and C. Webb, "Real-time modal synthesis of nonlinearly interconnected networks," in *Proc. Digital Audio Effects (DAFx-23)*, (Copenhagen, Denmark), 09 2023.

[11] S. Bilbao, C. Webb, Z. Wang, and M. Ducceschi, "Real-time gong synthesis," in *Proc. Digital Audio Effects (DAFx-23)*, (Copenhagen, Denmark), 09 2023.

[12] N. H. Asmar, *Partial differential equations with Fourier series and boundary value problems*. Upple Saddle River, New Jersey: Prentice Hall, 2005.

[13] J. Sherman and W. J. Morrison, "Adjustment of an inverse matrix corresponding to a change in one element of a given matrix," *Ann Math Stat*, vol. 21, pp. 124–127, 1950.

[14] R. Russo, M. Ducceschi, and S. Bilbao, "Efficient simulation of the yaybahar using a modal approach," in *Proc. Digital Audio Effects (DAFx-23)*, (Copenhagen, Denmark), 09 2023.

[15] F. Blanc, C. Touzé, J.-F. Mercier, K. Ege, and A.-S. B. Ben-Dhia, "On the numerical computation of nonlinear normal modes for reduced-order modelling of conservative vibratory systems," *Mech. Syst. Signal Process.*, vol. 36, no. 2, pp. 520–539, 2013.